Low-Field Magnetic Resonance

M. A. GARSTENS AND J. I. KAPLAN
United States Naval Research Laboratory, Washington, D. C.
(Received March 24, 1955)

Low-field magnetic resonance has been investigated for linearly and circularly polarized radio-frequency radiation for both the saturated and unsaturated case using modified Bloch equations for both. For the circularly polarized case, a quantum-mechanical solution is presented. Experimental verification for the linearly polarized case has been obtained.

INTRODUCTION

IN previous papers[1,2] we have investigated low-field magnetic resonance for linearly polarized radio-frequency radiation using power sufficiently weak not to cause saturation. We now consider what happens when the rf source is intense. To do this, we use modified Block equations,[3] allowing the relaxation to occur along and at right angles to the instantaneous external magnetic field. This method is applied to both the linearly and circularly polarized cases. In the latter case a quantum mechanical solution is also presented.

LINEARLY POLARIZED CASE

If the Bloch equations[4] are modified[3] so that longitudinal relaxation takes place along the field which is the resultant of the steady state field H_0 and the instantaneous radio-frequency field, and the lateral relaxation at right angles to it, we obtain the following equations of motion:

$$\dot{M}_x=\gamma M_y H_0-(M_x-\chi_0 H_1\cos\omega t)/\tau, \tag{1a}$$

$$\dot{M}_y=\gamma M_z H_1\cos\omega t-\gamma M_x H_0-M_y/\tau, \tag{1b}$$

$$\dot{M}_z=-\gamma M_y H_1\cos\omega t-(M_z-H_0\chi_0)/\tau, \tag{1c}$$

where γ is the gyromagnetic ratio, M_x, M_y, M_z the x, y, and z components of the magnetization, $H_1\cos\omega t$ the oscillating magnetic field in the x direction, τ the relaxation time, and ω the rf frequency. At low fields and for strong interactions, a single parameter τ characterizes both longitudinal and lateral relaxation times. We seek the steady-state solutions of Eqs. (1) under the assumption that $\bar{M}_z$ is time-independent, where $\bar{M}_z$ is the average value of M_z over one cycle of the rf field. Let

$$\begin{aligned} M_x&=A_1\cos\omega t+B_1\sin\omega t,\\ M_y&=A_2\cos\omega t+B_2\sin\omega t. \end{aligned} \tag{2}$$

From the above assumptions, substituting (2) in (1c) and averaging over one cycle, we get

$$0=-\tfrac{1}{2}\gamma H_1 A_2-(\bar{M}_z-H_0\chi_0)/\tau.$$

Therefore,

$$\bar{M}_z=H_0\chi_0-\tfrac{1}{2}\gamma H_1\tau A_2. \tag{3}$$

Substituting (2) and (3) back into (1), we obtain

$$\begin{aligned} -\omega A_1+B_1/\tau-\omega_0 B_2&=0,\\ A_1/\tau-\omega_0 A_2+\omega B_1&=\chi_0 H_1/\tau,\\ -\omega A_2+\omega_0 B_1+B_2/\tau&=0,\\ \omega_0 A_1+(\tfrac{1}{2}\gamma^2 H_1^2\tau^2+1/\tau)A_2+\omega B_2&=\gamma H_1 H_0\chi_0, \end{aligned} \tag{4}$$

where $\omega_0=\gamma H_0$.

The absorption χ'' corresponds to the out-of-phase component B_1 of M_x in (2). From Eq. (4), therefore,

$$\chi''=\frac{B_1}{H_1}=\chi_0\omega\tau\left((1+\omega^2\tau^2+\omega_0^2\tau^2)-\frac{4\omega_0^2\omega^2\tau^4}{(1+\omega^2\tau^2+\omega_0^2\tau^2)+\tfrac{1}{2}\gamma^2H_1^2\tau^2}\right)^{-1}. \tag{5a}$$

Figure 1 is a plot of χ'' against $\omega_0\tau$ for varying values of the saturation term $\frac{1}{2}\gamma^2H_1^2\tau^2$. For small values of this parameter compared to $1+\omega^2\tau^2+\omega_0^2\tau^2$ (no saturation), χ'' reduces to the well-known formula previously derived[1]:

$$\chi''=\tfrac{1}{2}\chi_0\omega\tau\left(\frac{1}{1+(\omega_0-\omega)^2\tau^2}+\frac{1}{1+(\omega_0+\omega)^2\tau^2}\right). \tag{6}$$

This appears in Fig. 1 as the upper curve marked unsaturated. As the rf power increases, we obtain the successive lower curves indicated, until at a point of total saturation (very large H_1) χ'' approaches the limiting curve,

$$\chi''=\chi_0\omega\tau/(1+\omega^2\tau^2+\omega_0^2\tau^2), \tag{5b}$$

indicated as 100 percent saturated in the figure. It is of interest to note that all of the curves terminate at

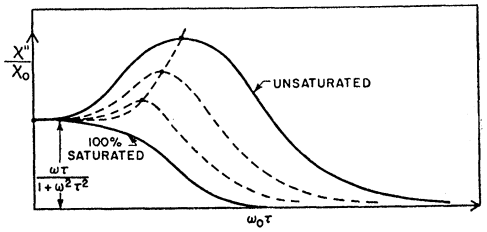

FIG. 1. Absorption in a coil oriented along the x axis for varying rf intensities.

[1] M. A. Garstens, Phys. Rev. **93**, 1228 (1954).
[2] Garstens, Singer, and Ryan, Phys. Rev. **96**, 53 (1954).
[3] Codrington, Olds, and Torrey, Phys. Rev. **95**, 607 (1954).
[4] F. Bloch, Phys. Rev. **20**, 460 (1946).

the same Debye value,

$$\chi''=\chi_0\omega\tau/(1+\omega^2\tau^2),$$

when $\omega_0=0$ and have the same zero slope at this point.

The maximum absorption points shift successively to the left with increasing saturation, approaching zero in the limit with 100 percent saturation.

The corresponding dispersion formula is given by

$$\chi'=\frac{A_1}{H_1}=\chi_0 \times\left\{\frac{1+\dfrac{(\frac{1}{2}\gamma^2H_1^2\tau^2+1+\omega_0^2\tau^2-\omega^2\tau^2)\omega_0^2\tau^2}{\frac{1}{2}\gamma^2H_1^2\tau^2+(1+\omega^2\tau^2+\omega_0^2\tau^2)}}{(1+\omega^2\tau^2+\omega_0^2\tau^2)-\dfrac{4\omega_0^2\omega^2\tau^4}{\frac{1}{2}\gamma^2H_1^2\tau^2+(1+\omega^2\tau^2+\omega_0^2\tau^2)}}\right\}. \quad (7a)$$

For low rf levels ($\frac{1}{2}\gamma^2H_1^2\tau^2\ll 1+\omega^2\tau^2+\omega_0^2\tau^2$), this reduces to

$$\chi'=\chi_0\left\{\frac{1+\dfrac{(1+\omega_0^2\tau^2-\omega^2\tau^2)\omega_0^2\tau^2}{(1+\omega^2\tau^2+\omega_0^2\tau^2)}}{(1+\omega^2\tau^2+\omega_0^2\tau^2)-\dfrac{4\omega_0^2\omega^2\tau^4}{(1+\omega^2\tau^2+\omega_0^2\tau^2)}}\right\}. \quad (7b)$$

At zero field, these reduce to the Debye dispersion formula:

$$\chi'=\chi_0/(1+\omega^2\tau^2).$$

Figure 2 is a plot of Eq. (7) for varying degrees of saturation and for several values of $\omega\tau$. For large saturation values, Eq. (7) reduces to

$$\chi'=\chi_0\left(\frac{1+\omega_0^2\tau^2}{1+\omega^2\tau^2+\omega_0^2\tau^2}\right). \quad (8)$$

For each of $\omega\tau=0$, 1, and 20, the figure first shows the unsaturated curve Eq. (7b), a partially saturated curve indicated by the first arrow, and fully saturated curve Eq. (8) indicated by the second arrow.

We have been able to verify Eq. (7) for the unsaturated case by fitting curves of the type indicated in Fig. 2 to experimental data obtained at this Laboratory by Waddel.[5] These were dispersion measurements taken at 16.9 Mc/sec at low rf levels on diphenyl-picryl hydrazyl and tris-p-nitro phenyl methyl. The theoretical unsaturated curves for both cases fitted experimental dispersion curves over their entire range within experimental error. For the hydrazyl an $\omega\tau$ of 5.9 was found to fit the data while for the methyl radical $\omega\tau$ was equal to 19.2, yielding a τ of 0.06×10^{-6} for the former and 0.18×10^{-6} for the latter.

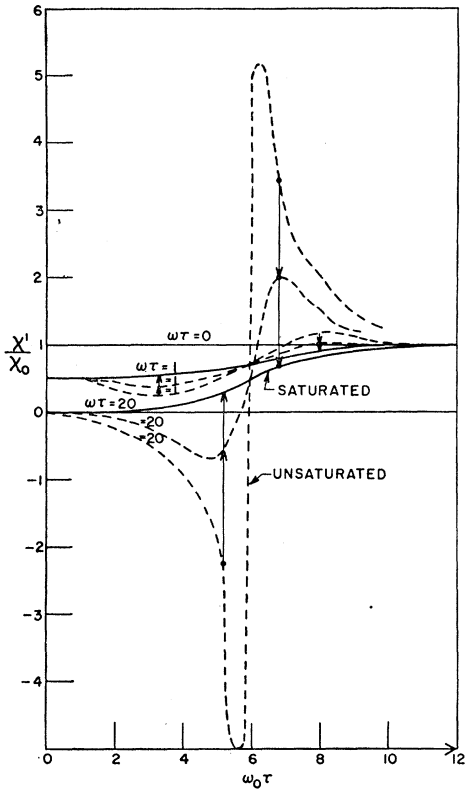

FIG. 2. Dispersion in a coil oriented along the x axis for varying rf intensities and values of $\omega\tau$.

In an attempt to obtain direct confirmation of low-field saturation effects at high rf levels an experiment was carried out using a Bloch type of apparatus with enough power to partially saturate diphenyl hydrazyl.

To obtain the χ'' and χ' values in this case, the M_y components of magnetization must be computed. Thus

$$\chi''=\frac{A_2}{H_1}=\frac{2\omega_0\omega^2\tau^3\chi_0}{[1+\tau^2(\omega_0-\omega)^2][1+\tau^2(\omega_0+\omega)^2]+\frac{1}{2}\gamma^2H_1^2\tau^2(1+\omega^2\tau^2+\omega_0^2\tau^2)}, \quad (9)$$

$$\chi'=\frac{B_2}{H_1}=\frac{2\omega_0\omega\tau^2\chi_0(\omega^2\tau^2-\omega_0^2\tau^2-1-\gamma^2H_1^2\tau^2)}{[1+\tau^2(\omega_0-\omega)^2][1+\tau^2(\omega_0+\omega)^2]+\frac{1}{2}\gamma^2H_1^2\tau^2(1+\omega^2\tau^2+\omega_0^2\tau^2)}. \quad (10)$$

These are shown plotted for increasing saturation in Figs. 3 and 4. Figure 5 shows some observed curves for χ' and χ'' at increasing saturation values using a detection coil at right angles to the rf coil.

[5] R. C. Waddel (private communication). Further publication on this is to appear.

$\bar{M}_z$ can be obtained from Eq. (3). Thus

$$\bar{M}_z=\chi_0\left\{H_0-\frac{\gamma^2\omega^2H_1^2\omega_0\tau^4}{[1+(\omega_0-\omega)^2\tau^2][1+(\omega_0+\omega)^2\tau^2]+\frac{1}{2}\gamma^2H_1^2\tau^2(1+\omega^2\tau^2+\omega_0^2\tau^2)}\right\}. \tag{11}$$

Of interest is the fact that $\bar{M}_z$ can have negative values for certain values of magnetic field, frequency and relaxation time.

CIRCULARLY POLARIZED CASE

The circularly polarized case has been solved by two methods, one in a manner similar to the previous case, the other, quantum mechanically.

(a) Classical Solution

If the equations of motion are modified to describe a circularly polarized rf, we obtain

$$\dot{M}_x=\gamma[M_yH_0+M_zH_1\sin\omega t]-(M_x-\chi_0H_1\cos\omega t)/\tau,$$
$$\dot{M}_y=\gamma[M_zH_1\cos\omega t-M_xH_0]-(M_y+\chi_0H_1\sin\omega t)/\tau,$$
$$\dot{M}_z=\gamma[-M_xH_1\sin\omega t-M_yH_1\cos\omega t]-(M_z-\chi_0H_0)/\tau.$$

The average value of M_z for the steady-state solution now becomes $\bar{M}_z=H_0\chi_0-\frac{1}{2}\gamma\tau H_1(B_1+A_2)$, and

$$\chi''=\frac{B_1}{H_1}=\frac{\chi_0\omega\tau}{1+(\omega_0-\omega)^2\tau^2+\gamma^2H_1^2\tau^2},$$
$$\chi'=\frac{A_1}{H_1}=\chi_0\frac{1+\omega(\omega_0-\omega)\tau^2+\gamma^2H_1^2\tau^2}{1+(\omega_0-\omega)^2\tau^2+\gamma^2H_1^2\tau^2};$$

also

$$\bar{M}_z=\chi_0\left(H_0-\frac{\gamma H_1^2\omega\tau^2}{1+(\omega_0-\omega)^2\tau^2+\gamma^2H_1^2\tau^2}\right).$$

As in the linearly polarized case, we note that $\bar{M}_z$ can take on negative values at low fields.

(b) Quantum-Mechanical Solution

In this method the spin resonance equations for the circularly polarized case are solved under the following assumptions:

(a) The system can be described by one relaxation time τ.

(b) That immediately after a collision the spin will achieve equilibrium with the resultant magnetic field at the time of the collision.

(c) That the rf field is monochromatic and of a constant value over the sample (i.e., no skin effects).

The solution of the time dependent Schrödinger equation for a spin $\frac{1}{2}$ particle acted on by a magnetic field **H** whose components are $H_1\cos\omega t$, $-H_1\sin\omega t$, and H_0, has been solved by Archibald[6] in a simple form. He finds that the ratio of the components of the spin wave function $\binom{a_+}{a_-}$ is given as

$$a_+/a_-=fe^{i\omega t}, \tag{12}$$

where

$$f=-(1/\omega_1)\{\alpha-i\Delta\tan[(t-t_0)\Delta/2+b]\},$$

$\alpha=\omega-\omega_0$, $\omega_1=\gamma H_1$, $\Delta^2=\alpha^2+\omega_1^2$, and b is an integration constant. By using this solution of the wave function, the expectation value of the three Pauli spin vectors is found to be

$$\langle\sigma_x\rangle=\frac{e^{-i\omega tf^*}+e^{i\omega tf}}{1+ff^*},$$
$$\langle\sigma_y\rangle=i\frac{[-e^{-i\omega tf^*}+e^{i\omega tf}]}{1+ff^*}, \tag{13}$$
$$\langle\sigma_z\rangle=\frac{f^*f-1}{1+ff^*}.$$

The value for the integration constant b is chosen so that just after a collision at time t_0 the components of the spin vector will be equal to the direction of the magnetic field at the time t_0. Thus we find that

$$\langle\sigma_x\rangle_{t=t_0}=H_1\cos\omega t_0/(H_1^2+H_0^2)^{\frac{1}{2}}, \tag{14a}$$
$$\langle\sigma_y\rangle_{t=t_0}=-H_1\sin\omega t_0/(H_1^2+H_0^2)^{\frac{1}{2}}, \tag{14b}$$
$$\langle\sigma_z\rangle_{t=t_0}=H_0/(H_1^2+H_0^2)^{\frac{1}{2}}=z. \tag{14c}$$

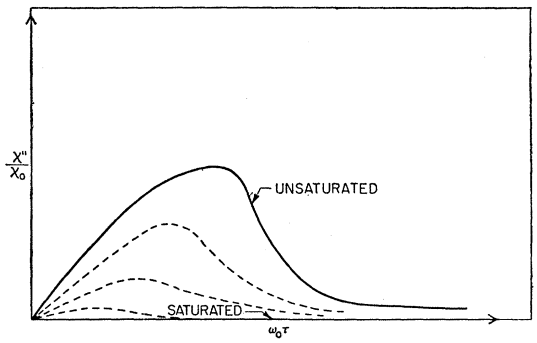

FIG. 3. Absorption in a coil oriented along the y axis for varying rf intensities.

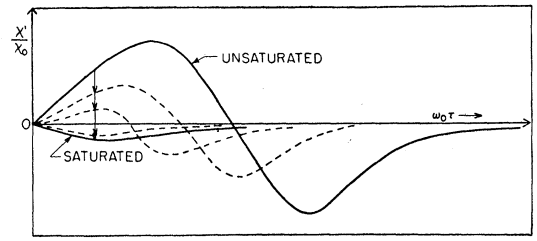

FIG. 4. Dispersion in a coil oriented along the y axis for varying rf intensities.

[6] J. Archibald, Am. J. Phys. **20**, 368 (1952).

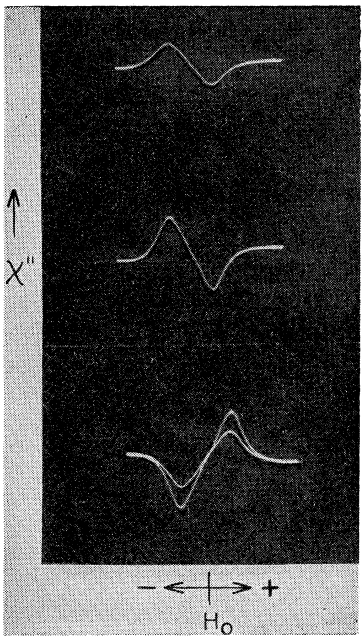

(a)

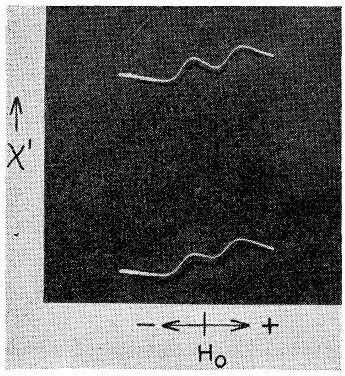

(b)

FIG. 5(a,b). Observed absorption and dispersion curves. These are to be compared with Figs. 3 and 4. With increasing rf intensity the absorption curves become flatter and the peak shifts towards zero field. The field H_0 is zero at the center of the curves increasing to the right and diminishing to the left. The third curve of 5(a) shows a saturated and unsaturated curve superposed.

It is seen from Eqs. (14)(a) and (b) that f must be real and from Eq. (14c) that

$$f=[(1+z)/(1-z)]^{\frac{1}{2}}=\delta. \tag{15}$$

We next write the integration constant b as a complex number $A+iB$ and then expand f as given in Eq. (12) into real and imaginary parts. The result is that

$$f=\frac{1}{\omega_1}\left[\left\{-\alpha-\frac{\Delta\tanh B(1+\tan^2 A)}{1+\tan^2 A\tanh^2 B}\right\}+i\left\{\frac{\Delta\tan A(1-\tanh^2 B)}{1+\tan^2 A\tanh^2 B}\right\}\right]. \tag{16}$$

The requirement that f must be real is satisfied by setting $\tan A=\infty$; then the real part becomes

$$f=(1/\omega_1)[-\alpha-\Delta\coth B]. \tag{17}$$

From Eqs. (15) and (17), the value of B is found to be

$$\coth B=-(1/\Delta)[\omega_1\delta+\alpha]. \tag{18}$$

All that remains to be done is to average $\langle\boldsymbol{\sigma}\rangle$ over all collision times t_0 by the prescription

$$\langle\langle\boldsymbol{\sigma}(\mathbf{t})\rangle\rangle=\int_{-\infty}^{t}\frac{e^{-(t-t_0)/\tau}}{\tau}\langle\boldsymbol{\sigma}(t-t_0)\rangle dt_0, \tag{19}$$

which is just the sum of contributions from all collision times t_0 weighted by an exponential law of decay. The final result for the x component is that

$$\langle\langle\sigma_x\rangle\rangle=-\frac{2\omega_1}{\varphi}\left\{\cos\omega t\left[\alpha\left(\frac{\frac{1}{2}\tau^2\Delta^2}{1+\Delta^2\tau^2}+\sinh^2 B\right)+\Delta(\sinh B\cosh B)\right]-\sin\omega t\left(\frac{\Delta}{2}\frac{\tau\Delta}{1+\tau^2\Delta^2}\right)\right\}, \tag{20}$$

where

$$\varphi=\Delta^2(2\sinh^2 B+1)+2\alpha\Delta(\sinh B\cosh B). \tag{21}$$

Substituting for $\cosh B$ and $\sinh B$ from Eq. (18) and recalling that the difference between the number of spin up and spin down states was assumed to be proportional to

$$\chi_0(H_1^2+H_0^2)^{\frac{1}{2}},$$

according to assumption (b), we have for the x component of magnetization

$$M_x=-\chi_0 H_1\omega\left[\cos\omega t\left(\frac{\alpha\tau^2}{1+\tau^2\Delta^2}-\frac{1}{\omega}\right)-\sin\omega t\left(\frac{\tau}{1+\tau^2\Delta^2}\right)\right]. \tag{22}$$

Identifying the in-phase component as the dispersion and the out-of-phase component as the absorption, we have that

$$\chi'=-\chi_0\left(\frac{\omega\alpha\tau^2}{1+\tau^2\Delta^2}-1\right), \tag{23}$$

and

$$\chi''=\chi_0\left(\frac{\omega\tau}{1+\Delta^2\tau^2}\right), \tag{24}$$

which are identical with the expressions obtained in the previous section. Equation (24) is identical with Bloch's[7] equation for absorption except that his ω_0 in the numerator is replaced by ω. This, of course, is a small effect except where ω varies appreciably in going through resonance. The dispersion on the other hand has an

[7] F. Bloch, Phys. Rev. **70**, 460 (1946).

added constant value χ_0 over the value derived by Bloch. Thus in the case of complete saturation the dispersion will have a constant finite value other than zero.

Further experimental work is planned to verify Eq. (5b) under conditions of complete saturation.

We are indebted to Dr. R. K. Wangness of the Naval Ordnance Laboratory for allowing us to see his manuscript on magnetic resonance for arbitrary field strength prior to publication. In this paper, the circularly polarized case has been worked out by a quantum-mechanical method different from that used here.

PHYSICAL REVIEW VOLUME 99, NUMBER 2 JULY 15, 1955

Multiple Resonances in Cobalt Ferrite*

P. E. TANNENWALD
Lincoln Laboratory, Massachusetts Institute of Technology, Lexington, Massachusetts
(Received April 1, 1955)

Double microwave resonances have been observed in cobalt ferrite when a magnetic field was applied in crystal directions near the hard axis. One resonance occurs before the magnetization vector is lined up with the external magnetic field and another occurs in the aligned state. The experimental results exhibit characteristic features expected before complete line-up and yield, at 90°C, $K_1/M=2200\pm200$ and $g=2.7\pm0.3$.

IN the past, microwave resonance experiments on ferromagnetic single crystals have been carried out on the assumption that the material was magnetized to saturation and the magnetization vector was fully aligned with the applied magnetic field. This is probably justified when the anisotropy field is of the order of 10 percent of the effective field necessary for resonance. Some materials, like cobalt ferrite, exhibit an anisotropy so large that at ordinary microwave frequencies the internal field puts the crystal already above resonance, according to the relation $\omega=\gamma H_{\text{eff}}$. However, as will be described now, the resonance frequency can be lowered by applying an external magnetic field in the hard direction of the crystal,[1] and furthermore, one resonance can be expected in the nonaligned state of the magnetization vector M and another in the aligned state.

Zeiger has given a general solution of the equation of motion[2] which includes the effects of anisotropy in terms of energy rather than effective demagnetizing factors. This has the advantage that it yields resonance conditions even when M is not lined up with the applied field. The results are shown for a cubic crystal on the assumption of single-domain structure, in Figs. 1 and 2, and clearly indicate the possibility of two resonances as a function of applied field H_0 in certain crystal directions.

Figure 3 shows the results of absorption measurements on a cobalt ferrite single crystal at 90°C as a function of magnetic field applied in various crystal directions Ψ in the (110) plane. The operating frequency (23 800 Mc/sec) is evidently above the "critical frequency" $\omega_c=2\gamma K_1/M$, because resonance was achieved in the easy axis ($\Psi=0°$) by application of an external field. A plot of the position of the high field peaks as a function of crystal orientation is shown in Fig. 4. This anisotropy curve, although similar, differs from that obtained in the usual effective demagnetizing theory.[3] As can be seen from Fig. 1, near the easy axis

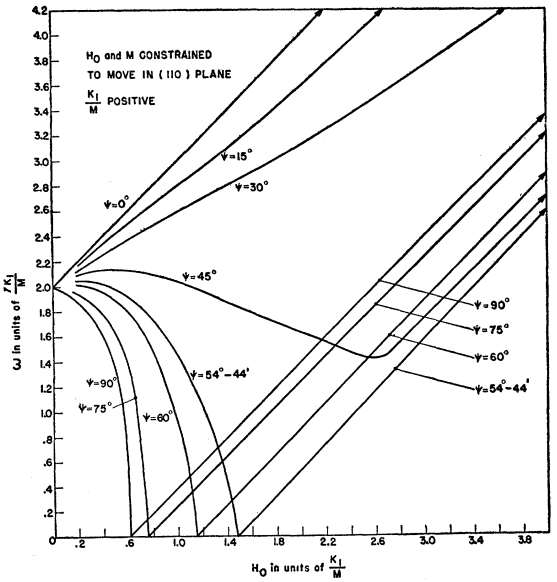

FIG. 1. Resonance condition in (110) plane. The microwave frequency ω is expressed in units of $\gamma K_1/M$ and external magnetic field H_0 is expressed in units of K_1/M.

* The research reported in this document was supported jointly by the Army, the Navy, and the Air Force under contract with the Massachusetts Institute of Technology.

[1] This idea is similar to that used by H. Suhl, Phys. Rev. **97**, 555 (1955) in achieving very-low-resonance frequencies in materials with low anisotropy.

[2] H. J. Zeiger, Lincoln Laboratory (unpublished notes). A similar solution was first given by J. Smit, Conference on Ferrimagnetism, October 11, 1954 (unpublished). See, also, reference 1.

[3] C. Kittel, Phys. Rev. **73**, 155 (1948).

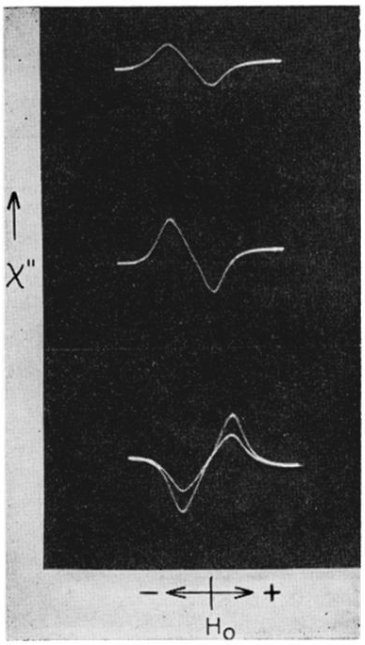

(a)

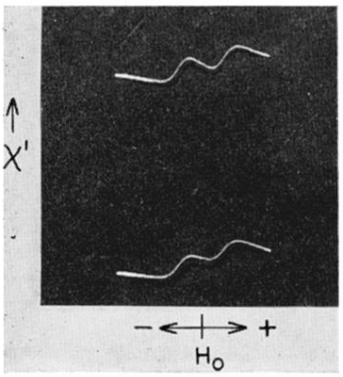

(b)

FIG. 5(a,b). Observed absorption and dispersion curves. These are to be compared with Figs. 3 and 4. With increasing rf intensity the absorption curves become flatter and the peak shifts towards zero field. The field H_0 is zero at the center of the curves increasing to the right and diminishing to the left. The third curve of 5(a) shows a saturated and unsaturated curve superposed.